Triazinylaniline derivatives as fluorescence probes. Part 3.[1,2] Effects of calcium and other metal ions on the steady-state and time-resolved fluorescence of bovine brain calmodulin labelled at lysine-75

David J. Cowley *,† and James P. McCormick

Department of Applied Physical Sciences, The University of Ulster, Coleraine, Northern Ireland, UK BT52 1SA

The fluorescence characteristics of bovine brain calmodulin labelled at lysine-75 by the reactive triazinylaniline (TA) dye *p*-$Et_2NC_6H_4C_3N_3(Cl)_2$ reveal structural changes critically dependent on calcium ion binding. Binding of two calcium ions to the C-terminal lobe exposes a hydrophobic region to the TA fluorophore, enhancing the fluorescence yield four-fold. Addition of two further calcium ions, to the N-terminal lobe, *decreases* the TA probe fluorescence three-fold by a displacement of the hydrophobic probe imposed by mutual interaction of two protein lobes/regions. The protein matrix induces circular dichroism in the attached TA dye in a calcium-dependent manner. Auxiliary binding of divalent metal ions at mmol dm^{-3} concentrations greatly enhances probe fluorescence. Despite the above changes the probe rotational relaxation times (8.0 ns) and limiting anisotropies (0.340) are insensitive to the calcium status of the triazinylaniline-labelled calmodulin (TACaM). Close co-rotation of the probe with a single lobe of the calmodulin carrier is likely, but the possibility of the TA probe optical transition axis lying parallel to a major axis of protein deformations is not excluded. Complex formation with melittin, and the potential utility of TACaM in the study of calmodulin-peptide interaction kinetics, are described.

Introduction

Calmodulin is a ubiquitous and highly conserved intracellular protein of 148 amino acid residues, which activates a number of enzymes in a calcium-dependent manner.[3-6] The structural implications of calcium binding to calmodulin, which results in a dramatic increase in affinity for the target proteins, have been much investigated by physical methods[3,6-8] including calorimetry, NMR, Raman, circular dichroism, fluorescence, small-angle X-ray and neutron scattering.

X-ray crystallographic studies (reviewed in ref. 6) of the calcium-saturated form of the protein reveal a dumbbell structure with two helix-loop-helix EF-hand binding sites for calcium in each of the discrete N- and C-terminal globular domains. These in turn are linked by an extended, solvent-exposed 26-residue central alpha helix. By contrast X-ray small-angle scattering data for calmodulin in solution (reviewed in ref. 7) are consistent with the size and shape of the globular domains determined in the crystal but indicate a 0.5–1.0 nm shorter distance between the lobes, suggesting that the central helix is kinked and may act as an 'expansion joint' to allow interdomain interaction. The 'flexible tether' model[9,10] is supported by optical[8] and heteronuclear multidimensional NMR[7] studies. The previously scant knowledge of the more compact but mobile structure of calcium-free (apo-) calmodulin[3,11] has been much advanced by multidimensional NMR studies.[12-14] These have also defined the major conformational rearrangements, including the exposure of the hydrophobic interior of the four-helix bundle, on uptake of calcium.

In binding sizeable peptides and proteins a high degree of co-operativity between hydrophobic patches in both domains of calmodulin, exposed on uptake of calcium ions, appears essential, as is confirmed by the significant alterations found in both calmodulin and target peptide structures from NMR[15,16] and X-ray[17,18] investigations of calmodulin complexes. The existence of an 'expansion' joint in the central region of calmodulin[19-20] appears to be a key to the low sequence specificity[21] but tight binding of calmodulin in the activation of target peptides and proteins following calcium uptake.

Plausible models exist for the docking of some peptidic substrates to calmodulin but the dynamic aspects of conformational transitions and domain interactions within calmodulin, both alone and when binding peptides, are less clear.[6,22-25]

Numerous studies exist on the kinetics and equilibria of metal ion binding to calmodulin and its tryptic fragments, including cadmium-113 NMR[26,27] and fluorescence stopped-flow kinetic experiments[28,29] which support the view that the two calcium-binding sites III and IV in the C-terminal domain possess a ten-fold (or more) greater affinity than the two sites I and II in the N-terminal domain. Within a domain a co-operativity exists[30] which is influenced by inter-domain interactions[31] and readily perturbed by mutations.[32-36] The co-operativity of calcium binding can be influenced allosterically by magnesium binding,[37,38] and auxiliary binding[39,40] of calcium and other divalent metal ions (*i.e.* above, and much weaker than, the binding at the four capital sites) exerts some influence. The sequential order/co-operativity of conformational changes in calmodulin on binding of calcium has been probed by the use of fluorescent single tryptophan mutants.[41] The intrinsic fluorescence of tyrosines 99 and 38 in the native calmodulins has been used to study the molecular hydrodynamics.[42-44]

Extrinsically-labelled fluorescent calmodulins have also found some applications. Energy transfer from terbium ions in wheat-germ calmodulin, labelled at cysteine-27 by an acceptor chromophore, allowed the elongation of the interdomain distance at lower pH (5.0) to be deduced.[45] Spinach calmodulins labelled at cysteine-26 by AEDANS[46] and by MIANS (and other sulfhydryl reactive dyes)[47] have signalled interactions with myosin light chain kinase, plasma membrane calcium pump peptide fragments,[46] and with caldesmon and

† *Present address:* Marion Merrell Research Institute Strasbourg, 16, rue d'Ankara, 67080 Strasbourg Cedex, France.

calcineurin,[47] respectively. Common fluorophores like dansyl *etc.* have been coupled specifically to (chemically-modified) tyrosines in calmodulin.[43] Labelling of bovine calmodulin with lysine-reactive reagents is less site-specific,[48-49] but such derivatives have proved useful in binding and kinetic studies of calmodulin-target peptide complexes.[50-53]

We report here on the basic steady-state and time-resolved fluorescence properties of bovine brain calmodulin specifically-labelled[54] at lysine-75 by a triazinylaniline (TA) reactive dye, fundamental to applications of this new, highly sensitive, fluorescent derivative of calmodulin (TACaM) to the kinetics and equilibria of interactions between calmodulin and target proteins. Complexation of TACaM by smooth muscle myosin light chain kinase, and kinetics of displacements by calmodulin-binding peptides have been reported recently.[54,55]

The photophysical and rotational properties, in solution and in lipid membranes, of several fluorescent TA derivatives are well-characterized[1,2,56] and shown to be very responsive to the microenvironment of the TA probe.

In triazinylaniline-labelled calmodulin (TACaM) the probe fluorescence yield varies more than four-fold in a distinctive pattern on uptake of calcium ions by the protein, which allows deductions concerning the accessibility of hydrophobic patches in both N- and C- terminal lobes, and of the mutual interaction of these lobes—a question of current interest. Furthermore, the strategic location of the TA probe enables conformational dynamics close to the crucial joint region of the central helix, as well as the general hydrodynamic properties, to be probed *via* the fluorescence anisotropy decay characteristics.

Experimental

Materials

Water was doubly-distilled and passed over Chelex 100 resin to remove residual calcium ions before use in preparation of buffers and stock solutions of EGTA or $CaCl_2$ (0.1 mmol dm^{-3}) from high grade materials.

Melittin (Sigma, 85% purity by HPLC) stock solutions were prepared by initial dissolution of the peptide in ethanol (< 10% of the final volume), followed by dilution with aqueous 0.1 mmol dm^{-3} Tris buffer, pH 8.

The dye *N*,*N*-diethyl-4-(dichloro-1,3,5-triazinyl)aniline was prepared and purified as described previously,[1] and dissolved in acetonitrile or dimethylformamide for use in the labelling experiments.

Calmodulin was purified from bovine brain[8] and fluorescent labelled in the presence of calcium ion (> 3 mmol dm^{-3}) by reaction with *N*,*N*-diethyl-4-(dichloro-1,3,5-triazinyl)aniline in 0.1 mol dm^{-3} Tris buffer at pH 8.5 and 22 °C in a manner previously described for the labelling of pig brain calmodulin.[55]

Under these conditions the labelling proceeds with 1:1 stoichiometry and selectively at residue lysine-75 to give a well-characterized adduct TACaM.[54]

Sample preparation for optical studies

Samples of TACaM for the combined circular dichroism–fluorescence titration studies (requiring prior knowledge of the initial calcium loading, high concentration of TACaM and the minimization of unlabelled protein concentration) were freshly prepared using higher concentrations than normal of both calmodulin and triazinylaniline dye reagent (the latter in three-fold excess) in order to achieve > 90% labelling efficiency. High specificity of labelling (at lysine-75) was ensured by the presence of high concentrations of calcium ion (> 3 mmol dm^{-3}) during the labelling reaction. Gel chromatographic elution (G25 Sephadex) of the labelled calmodulin using low calcium content buffer (*e.g. ca.* 50 μmol dm^{-3}), removed hydrolysed and unreacted dye and yielded TACaM saturated with calcium ions at the presumed four principal (capital) calcium binding sites, with a low percentage of unreacted calmodulin which does not absorb at the wavelengths (λ 350–380 nm) used to excite the TA label fluorescence.

For general fluorescence studies *e.g.* time-resolved fluorescence and anisotropy decay measurements, more dilute samples of TACaM (100–1000 mmol dm^{-3}) initially of stoichiometry 4 Ca^{2+}, TACaM after gel chromatography with eluent solution of low calcium concentration (20–100 μmol dm^{-3}) were titrated with EGTA solution to achieve a stoichiometry of 2 Ca^{2+}, TACaM by maximization of the TA label fluorescence intensity, on the basis of the titration curve determined absolutely at high concentrations of TACaM in separate experiments (see Fig. 2, Results). Apo-TACaM and auxilliary-site loaded TACaM were obtained by addition of excess EGTA or calcium chloride stock solutions, respectively.

For most experiments Tris buffer (occasionally Bis–Tris) was used to achieve a solution pH 7.5 to 8, but to facilitate acquisition of the CD spectra an *N*-ethylmorpholine buffer (40 mmol dm^{-3}, pH 8.4) was used to reduce the background correction in case measurements at the shorter UV wavelengths were required.

Methods

Near-UV circular dichroism spectra of TACaM solutions in quartz cuvettes of 10 mm optical path were recorded at 295 K using a Jasco J-600 spectropolarimeter. The instrument time constant was 1 s and five scans were averaged, with a small amount of smoothing, for each reported spectrum. The corresponding steady-state fluorescence spectra were recorded using a SPEX FluoroMax fluorimeter for the same solutions with a 4 mm excitation path length.

Steady-state fluorescence spectra were measured on either a Perkin-Elmer MPF-44B fluorometer or a SPEX FluoroMax for solutions in thermostatted 10 × 10 mm quartz cuvettes, of optical densities < 0.06 at the excitation wavelength (360 nm) with excitation and emission bandwidths of 4 nm. For quantum yield determinations emission spectra of TACaM were corrected by, and referenced to, quinine hydrogensulfate emission (Φ_F = 0.54). Time-resolved fluorescence data were acquired using the single-bunch mode beam facilities at the HA12 port of the synchrotron radiation source at SERC, Daresbury, and the lifetime and anisotropy decay analyses performed using the in-house programmes, as previously described for the investigation of TA fluorescence probes in phospholipid membranes.[2] For excitation of TACaM a wavelength of 360–370 nm was chosen; the emission was detected by a Mullard XP2020 photomultiplier tube with conventional single photon counting electronics, after passage through an analysing polariser and either a 400 nm cut-off filter or an 8 nm bandpass interference filter centered on 436 nm (occasionally 404 nm was examined).

Results

(I) General fluorescence properties of $n$$Ca^{2+}$,TACaM

The position of the fluorescence band maxima and the quantum yield of fluorescence of the triazinylaniline-labelled calmodulin (TACaM) are highly dependent on the calcium loading of the protein and its interaction with peptides such as melittin (Table 1).

(a) Radiative rate constants and emission band positions. Using the mean fluorescence lifetimes derived from a full three exponential analysis of fluorescence decays (see Table 2) the radiative and non-radiative rate constants have been calculated (Table 1).

For the complex of TACaM with the 29 amino acid residue peptide melittin, in the presence of high concentration of calcium ion, the radiative rate constant of the triazinylaniline fluorophore (3.39×10^8 s^{-1}) equals the Strickler-Berg estimate of 3.4×10^8 s^{-1} calculated on the basis of the UV absorption band of TACaM centred on 365 nm (molar extinction

coefficient 40 500 dm^3 mol^{-1} cm^{-1}); this value has also been found for related (amino-substituted) triazinylaniline compounds (see Table 1 in ref. 1) and implies a very hydrophobic environment for the TA probe in the TACaM–melittin complex since this magnitude of radiative rate constant is only obtained for TA derivatives in non-polar organic solvents such as toluene. In polar, and especially in aqueous media, k_F is lowered considerably towards 1×10^8 s^{-1} as is observed here for TACaM in the absence of bound calcium ions.

As expected, the emission wavelength maxima is blue-shifted as the polarity of the microenvironment of the TA fluorophore decreases, while the quantum yield of fluorescence (Table 1) and the mean fluorescence lifetime (Table 2) increase.

(b) Fluorescence decay times. While two exponential terms provided a reasonable fitting to the observed fluorescence decay profiles (see Fig. 1 for typical impulse and emission response curves) three exponential fits were superior. Although not using global constraints in the data analysis, constant lifetime components of *ca.* 2.2, 1.1 and 0.2 ns appear to be present (Table 2), whose contributions change significantly with the calcium loading status of TACaM. The shortest component is relatively insignificant (fractional intensity $f_1 < 10\%$), except for calcium-free (apo)TACaM.

The mean fluorescence lifetimes were moderately sensitive to temperature (full data and analyses not shown); typically, for the 4 Ca^{2+}, TACaM species in Bis-Tris buffer at pH 7.0, the lifetime decreased linearly from 1.60 ns at 285 K to 1.26 ns at 313 K, a rate of change of 0.83% K^{-1}.

At 298.5 K for the same species in Bis-Tris buffer the mean fluorescence lifetime was 1.31, 1.45, 1.58 and 1.44 ns at solution pH 5.93, 6.97, 8.07 and 9.04, respectively.

(c) Effects of calcium-TACaM stoichiometry on circular dichroism and fluorescence spectra. Fig. 2 shows the variation in the intensity of TA probe fluorescence at 412 nm of a concentrated solution of TACaM (43 mol dm^{-3}) in *N*-ethylmorpholine buffer (40 mmol dm^{-3}, pH 8.4), on titration with a buffered solution of EGTA (1 mmol dm^{-3}). Circular dichroic absorption spectra (Fig. 3) were also measured concurrently at selected key points on the fluorescence titration curve. Retrospectively calculated [calcium]/[TACaM] ratios were 0, 0.28, 1.21, 2.14, 3.07 and 4.0 at which the calculated differential CD molar extinction coefficients were +1.07, +0.39, −2.30, −3.95, −4.05 and −3.98 dm^3 mol^{-1} cm^{-1}, respectively, for an absorption wavelength of 370 nm at which only the TA chromophore absorbs. Repetitions of the

Table 1 Fluorescence properties of TACaM species in aqueous Tris buffer (0.1 mol dm^{-3}, pH 7.5) at 296 K[a]

System	Q_F	λ_{max}/nm	$k_F/10^8$ s^{-1}	$k_{NR}/10^8$ s^{-1}
0 Ca^{2+} (EGTA)	0.085	422	0.80	8.63
2 Ca^{2+}	0.34	413	2.06	4.00
4 Ca^{2+}	0.13	418	0.86	5.72
Excess Ca^{2+}	0.37	412	2.32	3.95
Melittin, excess Ca^{2+}	0.65	406	3.39	1.90
Melittin, EGTA	0.275	405	1.42	3.73

[a] Q_F is the fluorescence quantum yield determined by reference to quinine hydrogensulfate in 0.5 mol dm^{-3} sulfuric acid ($Q_F = 0.54$) for 350 and 360 nm excitation wavelengths using a TACaM concentration of 1.15 μmol dm^{-3}. Excess Ca^{2+} concentration was *ca.* 1 mmol dm^{-3}. The radiative (k_F) and non-radiative (k_{NR}) rate constants of decay are calculated from the quantum yields using the mean fluorescence lifetimes given in Table 2.

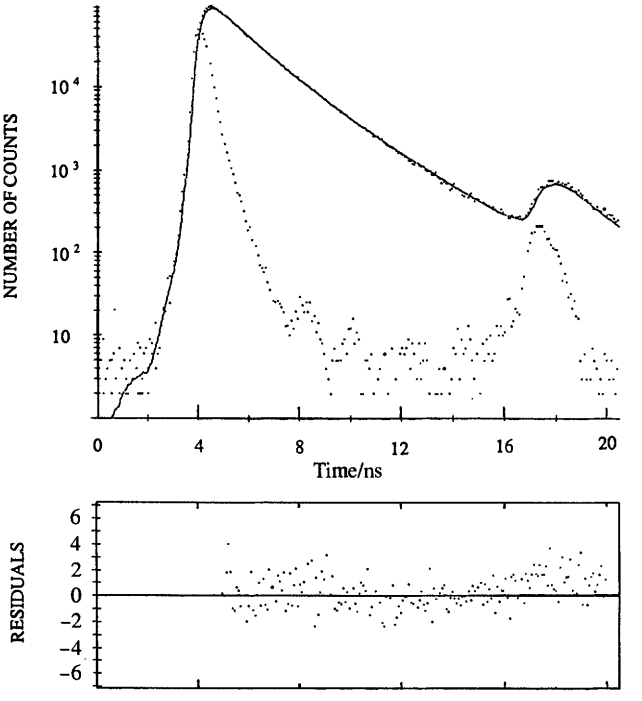

Fig. 1 Typical fluorescence excitation and emission decay profiles. TACaM (concentration ~ 2 μmol dm^{-3}) in Tris buffer (pH 7.5, 296 K) in the presence of excess calcium ions (0.67 mmol dm^{-3}). Excitation wavelength 360 nm; emission was detected after passage through a 436 nm interference filter (bandpass 8 nm). The impulse curve maximum is at 4.10 ns. The solid line, and the residuals, pertain to a fitting using a two exponential fluorescence decay model.

Table 2 Fluorescence lifetime analyses for TACaM[a]

Calcium loading	τ_1/ns	f_1 (%)	τ_2/ns	f_2 (%)	τ_3/ns	f_3 (%)	Mean τ/ns	n
(i) 0 Ca^{2+} (EGTA)	2.36	26.1	0.99	40.2	0.16	33.6	1.06	6
	±0.14	4.7	0.10	1.5	0.01	3.9		
(ii) 2 Ca^{2+}	2.24	54.0	1.15	38.0	0.12	8.0	1.65	1
(iii) 4 Ca^{2+}	2.25	45.0	1.10	45.0	0.16	10.0	1.52	6
	±0.06	3.8	0.05	3.0	0.013	1.6		
(iv) Ca^{2+} (excess)	2.29	41.6	1.24	50.0	0.26	8.4	1.595	6
	±0.04	2.2	0.04	1.5	0.04	1.5		
(v) Ca^{2+} (excess) + melittin	2.15	77.6	1.03	20.9	0.20	1.5	1.89	1
(vi) 0 Ca^{2+} (EGTA) + melittin	2.63	56.0	1.24	38.0	(3.72)	6.0	1.94	1

[a] f_i = fractional intensity of lifetime component τ_i; n = number of independent determinations. Excitation wavelengths 360 and 370 nm; emission detected using 8 nm band pass interference filters centred on 404 and 436 nm, and also 400 nm cut-off filter (no significant differences or trends in lifetime analyses were found for a given chemical system). [TACaM, 4 Ca^{2+}] = 2.0 to 2.2 μmol dm^{-3} [except for (ii) and (vi), in Tris buffer (0.1 mol dm^{-3}, pH 7.5, 296 K)]. (i) [EGTA] = 42 μmol dm^{-3}. (ii) [TACaM, 4 Ca^{2+}] = 10.8 μmol dm^{-3}; titrated with EGTA solution (2.86 mmol dm^{-3}) while monitoring fluorescence intensity. (iii) Net added [Ca^{2+}] = 30 μmol dm^{-3}. (iv) Excess [Ca^{2+}] = 0.7 to 0.9 mmol dm^{-3}. (v) Excess [Ca^{2+}] = 0.7 mmol dm^{-3}, [melittin] = 2.3 μmol dm^{-3}. (vi) [EGTA] = 56 μmol dm^{-3}, [melittin] = 11.5 μmol dm^{-3}, [TACaM] = 11 μmol dm^{-3}.

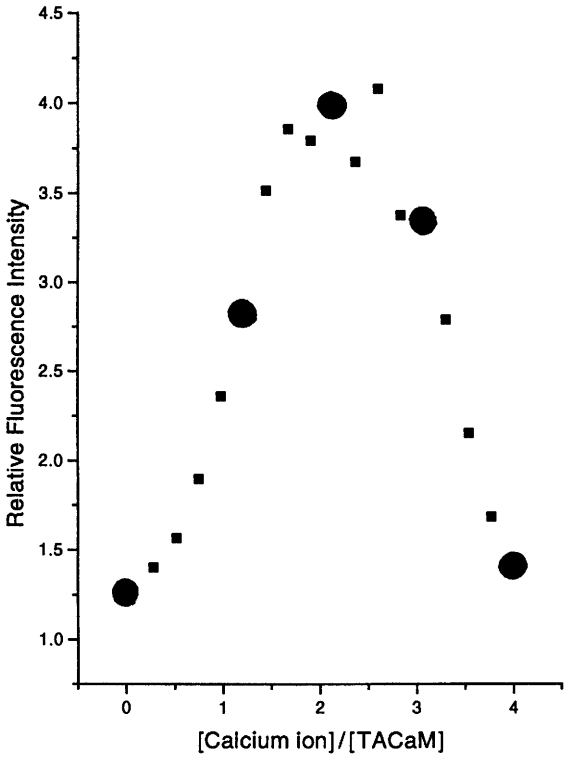

Fig. 2 Variation of the relative fluorescence intensity at 412 nm emission wavelength of TACaM with the mean calcium loading of the labelled protein for excitation at 365 nm. The bound calcium was varied by titration of a sample of 4 Ca^{2+}, TACaM (concentration 43 μmol dm^{-3}) with EGTA solution (1 mmol dm^{-3}). Large solid circles indicate the samples for which circular dichroism spectra were recorded concurrently (see Fig. 3). The buffer was *N*-ethylmorpholine (40 mmol dm^{-3}, pH 8.4, 295 K).

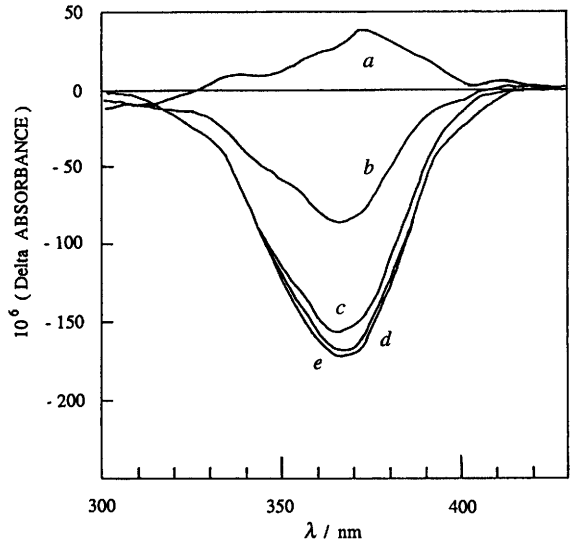

Fig. 3 Circular dichroism spectral curves for TACaM (43 μmol dm^{-3}) in *N*-ethylmorpholine buffer (40 mmol dm^{-3}, pH 8.4, 295 K) at mean stoichiometric ratios [calcium ion]/[TACaM] of (*a*) 0.0, (*b*) 1.21, (*c*) 2.14, (*d*) 3.07, (*e*) 4.00. Fluorescence characteristics of these samples were determined concurrently (see Fig. 2).

fluorescence titration experiment under a variety of conditions of TACaM concentrations, buffer type and concentration, addition of EGTA or calcium *etc.*, confirmed the same general profile as that shown in Fig. 2, and which is nearly symmetrical about a [calcium]/[TACaM] ratio of 2:1. This profile was used to obtain TACaM species of defined (average) calcium stoichiometry by fluorimetric titration of solutions too dilute

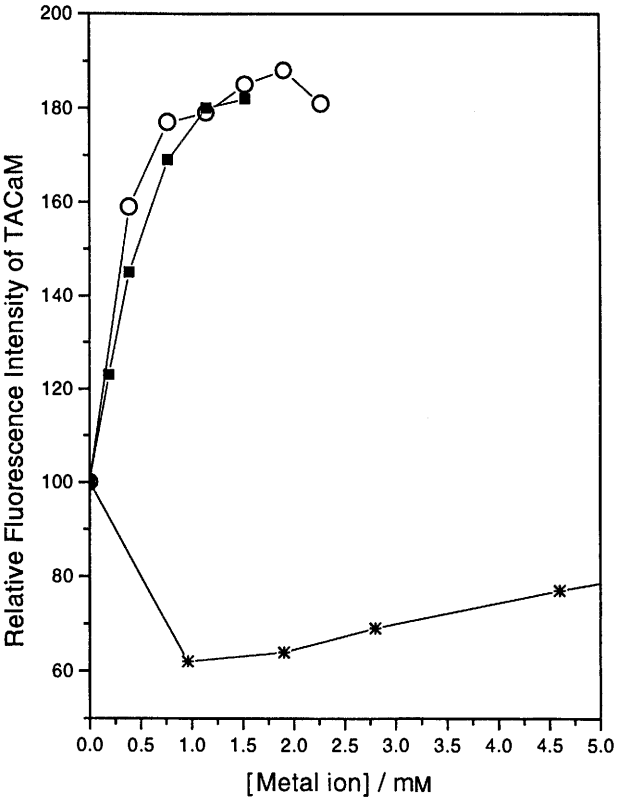

Fig. 4 Variation of relative fluorescence emission intensity of TACaM (at low μmol dm^{-3} concentrations) in Tris buffer (50 mmol dm^{-3}, pH 8.0, 295 K) with metal ion binding at primary and secondary binding sites. Excitation at 365 nm, emission at 412 nm. Open circle: Cd^{2+} ion; filled square: Zn^{2+} ion; star: Mn^{2+} ion.

(< 100 nmol dm^{-3}) to manipulate with certainty *via* additions of absolute concentrations of calcium or EGTA chelator.

(d) Secondary metal ion binding. At high absolute concentrations of calcium (of 0.5 mmol dm^{-3} and above) further secondary binding of metal ion occurs which also results in an increase in fluorescence intensity from that observed at a Ca^{2+}/TACaM ratio of 4. In the limit of [Ca^{2+}] > 5 mmol dm^{-3} the fluorescence intensity is greater than that seen when this ratio is 2, *i.e.* at the maximum of the curve in Fig. 2. Table 1 provides a concise quantitative summary.

Metal ions other than calcium may influence the fluorescence quantum yield of TACaM *via* secondary, and in some cases primary, binding to the protein. Fig. 4 depicts the changes in intensity of the emission from low calcium solutions initially containing the 4 Ca^{2+}, TACaM species, on addition of mmol dm^{-3} concentrations of Zn^{2+}, Cd^{2+} and Mn^{2+} ions.

Table 3 includes mean fluorescence lifetimes for these systems, at the chosen concentration limits, which correlate well with the steady-state fluorescence intensities. Qualitatively, zinc and cadmium ions appear to mimic the action of calcium; the effect of manganous ion is more complex.

(II) Fluorescence anisotropy decays

The fluorescence anisotropy decay characteristics of TACaM in the presence of calcium, other metal ions, and of the bee venom peptide melittin were determined in order to gain insight, *via* the rotational relaxations, into the structural changes in the protein in general, and those associated with the central helix in particular, as a result of metal ion/ligand binding.

Good anisotropy decay profiles were obtained for all samples from a time corresponding to the rising edge of the excitation pulse (*e.g.* 1% of the maximum pulse counts) to 15 ns after the pulse (representing *ca.* 10 mean fluorescence lifetimes). The anisotropy decay curves were well fitted using a single exponential term (Fig. 5 gives an experimental curve and fit; Table 3 gives the extracted molecular rotational relaxation

Table 3 Rotational anisotropy decay analyses for TACaM[a]

System	Mean τ/ ns	Q_1 (rot)/ ns	$r(0)$
(i) 0 Ca^{2+} (EGTA)	1.06	8.19 ± 0.10	0.320 ± 0.006
(ii) 2 Ca^{2+}	1.65	7.90	0.34
(iii) 4 Ca^{2+}	1.52	8.14 ± 0.24	0.338 ± 0.009
(iv) Ca^{2+} (excess, 0.9 mmol dm^{-3})	1.595	8.80 ± 0.20	0.337 ± 0.012
(v) Ca^{2+} (excess) + melittin	1.89	10.5	0.343
(vi) 0 Ca^{2+} (EGTA) + melittin	1.94	(12)	0.324
(vii) 4 Ca^{2+}, Zn^{2+} (2.3 mmol dm^{-3})	2.03	8.0	0.334
(viii) 4 Ca^{2+}, Cd^{2+} (1.5 mmol dm^{-3})	1.94	8.0	0.345
(ix) 4 Ca^{2+}, Mn^{2+} (12.7 mmol dm^{-3})	1.65	(9.5)	0.33

[a] For (i)–(vi), see Table 2 footnote. For (vii)–(ix), excitation wavelength 360 nm; emission detected using 8 nm band pass interference filters centered on 436 nm. Residual [calcium] was *ca.* 60 μmmol dm^{-3}. [TACaM, 4 Ca^{2+}] = 2.0 to 2.2 μmol dm^{-3} [except for (ii) and (vi), in Tris buffer (0.1 M, pH 7.5, 23 C)]. (i) [EGTA] = 42 μmol dm^{-3}. (ii) [TACaM, 4 Ca^{2+}] = 10.8 μmol dm^{-3}; titrated with EGTA while monitoring fluorescence intensity. (iii) Net added [Ca^{2+}] = 30 μmol dm^{-3}. (iv) Excess [Ca^{2+}] = 0.7 to 0.9 mmol dm^{-3}. (v) Excess [Ca^{2+}] = 0.7 mmol dm^{-3}, [melittin] = 2.3 μmol dm^{-3}. (vi) [EGTA] = 56 μmol dm^{-3}, [melittin] = 11.5 μmol dm^{-3}, [TACaM] = 11 μmol dm^{-3}.

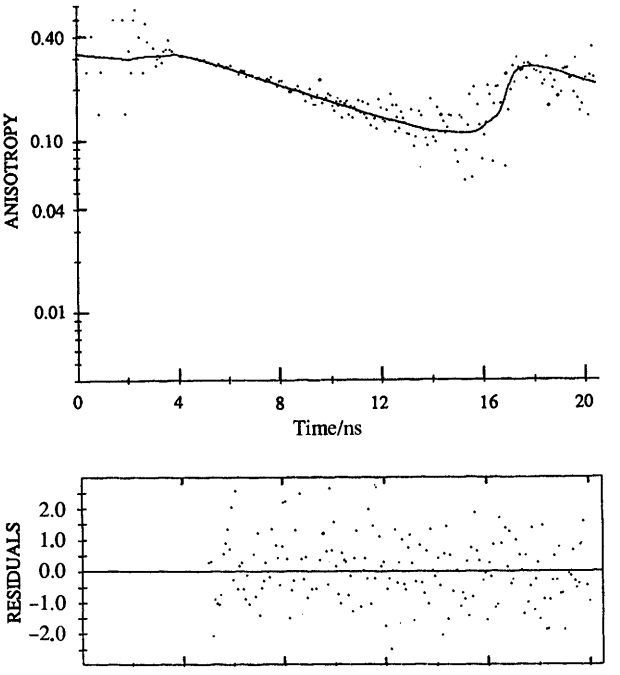

Fig. 5 Typical fluorescence anisotropy decay profile of TACaM. TACaM (concentration ~ 2 μmol dm^{-3}) in Tris buffer (pH 7.5, 296 K) in the presence of excess calcium ion (0.67 mmol dm^{-3}). Excitation wavelength 360 nm; emission was detected after passage through a 436 nm interference filter (bandpass 8 nm). The impulse curve maximum is at 4.10 ns. The solid line, and the residuals, pertain to a fitting using a non-associated model with a single rotational correlation time and a two exponential fluorescence decay.

times). The fluorescence anisotropy $r(t)$ decays towards zero from an initial value of 0.335 ± 0.01. For comparison, the steady-state fluorescence anisotropy of 0.34 measured for glycerol solutions of TA dye derivatives, analogous chromophorically to TACaM, approximates closely to the limiting anisotropy r_0 in the absence of molecular rotation.[2] The angle between the absorption and emission transition dipoles is small (18°),[56] as expected from the intramolecular charge-tranfer nature of the electronic transition and the relative location of electron donor and acceptor moieties in the molecular framework; this is a useful feature of the triazinylaniline fluorophore.

For TACaM under all conditions the TA label appears to be tightly anchored to the protein framework *i.e.* little, if any, independent motion of the probe occurs. The surprising feature of the derived rotation times is their constancy (φ = 8.0 ns), despite the structural realignments on change in calcium ion occupancy of the protein as evidenced by the dramatic alterations in the other photophysical properties of the reporter TA fluorophore. Here only complex formation of TACaM with melittin significantly alters the apparent rotation time, with a magnitude (10.5 ns) that conforms to expectations based on the additional mass of the melittin.‡

(III) Melittin–TACaM complex formation

Steady-state fluorescence parameters for TACaM in the presence of melittin are given in Table 1. Binding of melittin to apo-TACaM produces a stronger *relative* enhancement of the TA fluorescence quantum yield than does its binding to calcium-loaded TACaM. In both cases, however, melittin shields the TA fluorophore from the aqueous media with good efficiency. In the system TACaM–melittin–excess calcium the fluorescence properties of the TA probe are identical to those found for TA–amine derivatives in toluene, a dramatic indication of the extreme hydrophobicity of the pocket enclosing the TA probe. For a TACaM concentration of *ca.* 3 nmol dm^{-3} maximal changes in fluorescence band position (blue shift) and intensity were achievable with melittin concentrations of >4 nmol dm^{-3}. Thus the strong (<nmol dm^{-3}, K_d) affinity of melittin for 4 Ca^{2+}, TACaM is close to that noted for unlabeled calmodulin. The fluorescence emission at 406 nm of the TA fluorophore could be sensitized by excitation at 290 nm of the tryptophan residue 19 of the peptide only in the melittin–TACaM complex. The critical distance for resonance energy transfer, R_0, estimated from the large overlap integral of the melittin emission spectrum and the UV absorption spectrum of TACaM, is 2.5 nm. This magnitude of R_0 is comparable to or larger than the expected dimensions of the complex (radius of calmodulin ≈ 2.1 nm), and precludes the derivation of a meaningful internal distance between the TA and Trp fluorophores from the expected near 100% efficiency of energy transfer.

Discussion

1. The TA fluorophore is very responsive to changes in polarity of its microenvironment. In TA labelled calmodulin (TACaM) a complex but marked dependence on calcium uptake by the protein is observed, with a greater than four-fold ratio of maximum to minimum emission intensity (Fig. 2). This sensitivity confirms the strategic location of the TA probe, at lysine-75 close to the crucial 'expansion joint' of the central section, in monitoring the intra-protein interactions and mobility.

2. A major concern in the use of extrinsic fluorescent probes is the potential for significant perturbation of the native protein structure. In the case of TACaM the (desirable) converse appears to be true, as judged on the following grounds.

‡ A rotational relaxation time of 10.5 ns and a limiting anisotropy of 0.318 were determined for the complex between unlabelled calmodulin and melittin peptide labelled with the TA probe at a lysine residue. While the exact residue has not been determined at present, UV absorption data reveal a clean reaction (isosbestic point) and a 1:1 stoichiometry of dye to melittin.

(i) Homogeneous solutions of triazinylaniline derivatives of aliphatic amines, identical in spectroscopic and chemical terms to TA coupled to a protein at the ε-nitrogen of a lysine sidechain, do not exhibit circular dichroism. TACaM, however, does show circular dichroism at the optical absorption band of the triazinylaniline chromophore (~ 365 nm). This induced CD effect is attributable either to an asymmetric electronic distortion of the TA by the constraints of the surrounding protein matrix or more likely to an intensity-borrowing electronic exchange, promoted by proximity, involving the peptidic cumulative amide transition (strong CD) and the TA charge-transfer transition. In addition, the induced CD effect on the TA probe varies significantly (Fig. 3) with the calcium status of the calmodulin *i.e.* the protein imposes its transformations on the probe and not *vice versa.*

(ii) Similarily, the fluorescence quantum yield of the TA probe (which reflects the micropolarity of its surroundings) undergoes several strong alterations as a function of the calcium status of the protein *i.e.* the probe is steered and displaced from sites by the chaperone protein matrix. If the converse were to be true then the probe would remain fixed in its self-determined pocket and the fluorescence would be relatively constant.

3. The displacements of the TA probe as a result of intra-protein conformational adjustments and domain movements, and their relationship to the sequence and/or co-operativity of calcium binding to TACaM, are now examined in detail. The inverse correlation of fluorescence quantum yield and the wavelength of the emission band maxima, with the latter arising from environmental polarity changes, is obeyed without exception (Table 1). Thus it would be dubious to invoke simply an internal quenching mechanism without a major change in hydrophobicity of the environment in order to explain the strong decline in fluorescence intensity on passage from 2 Ca^{2+}, TACaM to 4 Ca^{2+}, TACaM (Fig. 2).

The low TA fluorescence yield in apo-TACaM, the band maxima at 422 nm, and the low value of the radiative rate constant k_F all indicate a moderate exposure of the dye probe to aqueous phase. Chemical and (photo)physical studies of the triazinylanilines in solution and heterogeneous systems, *e.g.* lipid bilayers and micelles, indicate a high propensity for the triazinyl moiety to seek hydrophobic locations when available. Thus in apo-TACaM the existence of highly hydrophobic regions or pockets *accessible to the TA probe* is most unlikely.

On filling of the two strong-binding calcium sites III and IV in the C-terminal lobe the effective environment polarity surrounding the TA probe is reduced considerably. This is consistent with the aromatic TA probe associating strongly with a hydrophobic patch on the C-terminal lobe exposed only on calcium uptake in that lobe.

The sigmoidal increase in fluorescence intensity for nominal calcium/TACaM stoichiometry change 0→2 is suggestive, but not proof, of a co-operative filling of calcium sites III and IV. (88% of the maximum intensity gain is realised at 1.5 Ca^{2+}/TACaM ratio; but note that fluorescence yields for all the individual species are not known).

Further increase in calcium level, in which filling of the weaker affinity sites I and II in the N-terminal lobe occurs, leads to a substantial decrease in fluorescence yield of the TA probe down to a level at 4 Ca^{2+}, TACaM which is nevertheless 1.5 times greater than that for apo-TACaM (Fig. 2). The change in probe fluorescence characteristics, with calcium filling 2→4, is not ascribable merely to a spontaneous switching of hydrophobic locations, for example to a freshly exposed hydrophobic patch on the N-terminal lobe, since the new position of the emission band maxima (at calcium filling of 4) indicates this to be energetically unfavourable with respect to the TA probe interactions *per se.* Rather the data suggest that the displacement of the hydrophobic TA probe to a more solvent-exposed region is driven by the calmodulin protein and arises from either strong inter-lobe, or at least central helix-single lobe, hydrophobic interaction(s). This is consistent with the findings of Meador *et al.* for binding of target peptides to calmodulin linker helix mutants that the major calmodulin-target structure is preserved at the expense of linker conformation.[19]

Overall the transformations seen for calcium filling 0→2→4 find a parallel in the rates of tryptic digestion of calmodulin at Arg-74, Lys-75 and Lys-77 in the central helix.[20] Whereas full occupancy of the four Ca^{2+} binding sites produces little change in the susceptibility of the central helix to proteolytic attack, binding of two Ca^{2+} produces a 10-fold enhancement ascribed to enhanced flexibility. One may speculate that in the case of the 2 Ca^{2+}, TACaM species such flexibility in the central region would permit a more efficient burial of the triazinylaniline fluorophore by hydrophobic patches of the major lobes.

4. At high absolute concentrations of calcium (> 0.5 mmol dm^{-3}) further secondary binding of metal ion occurs which also results in an increase in fluorescence intensity from that observed at a Ca^{2+}/TACaM ratio of 4. In the limit of $[Ca^{2+}] > 5$ mmol dm^{-3} the fluorescence intensity is even greater than that seen when this ratio is 2, *i.e.* at the maximum of the curve in Fig. 2. This situation is not relevant physiologically to the action of calmodulin but requires some explanation in the overall scheme.

In the vicinity of the labelled residue lysine-75 are several acidic residues (Asp-78, Asp-80, Glu-82, Glu-83, Glu-84). Lower affinity binding of metal ions (K_d in the mmol dm^{-3} range) at these acidic sites could neutralize the ionic charges, reduce the micropolarity with respect to the TA fluorescent label, and/or increase flexibility of the 'expansion joint' region which could in turn assist a better re-shielding of the TA probe, as noted above for the 2 Ca^{2+}, TACaM case.

Cadmium(II), known to substitute analogously for calcium in calmodulin, and zinc(II) ions give the same qualitative secondary binding effect as calcium (Fig. 4) whereas manganese(II) ions ($3d^5$, high spin configuration) appear to diminish the fluorescence yield, perhaps by a paramagnetic quenching mechanism. The metal ion association constants (for auxiliary ion binding) are similar, as would be expected for general complexation by sidechain carboxylate groups.

5. Despite the intriguing dependences of the fluorescence quantum yield on metal ion binding, both primary and secondary, the rotational relaxation times derived from fluorescence anisotropy decay analyses are conspicuous by their insensitivity to the conditions (Table 3); the values cluster closely around 8.0 ns. Similarily, the derived limiting anisotropy values r_0 at 0.3350 ± 0.005 are in good correspondance with the value determined for TA derivatives in glycerol solvent at low temperatures (0.34). The local, individual motion of the TA probe appears to be negligible, except in the case of apo-TACaM (± melittin), with depolarizing rotations restricted to those of the carrier protein. For a hydrated globular protein of MW 16 700, a rotational correlation time of 6.6 ns is calculated at 293 K.[44] A value of *ca.* 9.0 ns (293 K) is estimated, however, assuming an empirical ratio of 1.8 between observed rotational correlation times and those calculated from simple hydrodynamic theory for many proteins.[57] ^{15}N NMR investigations of the backbone dynamics of calcium-saturated calmodulin[7] have revealed the flexibility of the central tether and motional correlation times of 6.3 and 7.1 ns deduced for the independently tumbling C- and N-terminal lobes, respectively.

From the magnitude of the long rotational relaxation time (8.0 ns) the TA probe, and thus also parts of the amino acid sequence designated the 'central helix' to which it is attached, appears to be intimately co-rotating with at least one lobe of the calmodulin protein.

The complex changes in fluorescence yields have been interpreted earlier in terms of significant alterations in lobe conformations and interactions; thus changes in hydrodynamic dimensions and in the corresponding three intrinsic rotation

times of a non-spheroidal particle are anticipated. For consistency it must be postulated *either* that the TA probe is an insensitive reporter of these changes in rotation because its electronic transition axis remains orthogonal to the molecular rotation axis about which the major events take place (if indeed the probe is associated with the whole compact protein) *or* that the triazinylaniline fluorophore is strongly associated with one lobe for any given calcium loading of the calmodulin. The latter seems more reasonable in the face of the NMR evidence but the possibility that the fluorophore transition moment direction remains parallel to the direction of any major elongation or contraction of the protein is a feasible if disappointing feature of TACaM with respect to hydrodynamic investigations.

6. The 1:1 complex between calmodulin and melittin has been extensively studied.[58-60] Our results confirm the expected strong interaction between TACaM and melittin; tight association of TACaM with the peptide melittin in the presence of excess (0.9 mmol dm^{-3}) calcium ion, however, is revealed by the increase in the TA anisotropy decay time to 10.5 ns.

7. Because of the high molar extinction coefficient of the TA probe at 365 nm, and the good yield of fluorescence centred at 405–420 nm, low nanomolar concentrations of TACaM may be detected readily. Thus kinetic studies diagnostic of mechanism(s) for peptide interactions with calmodulin at nanomolar concentrations, for example conformational intermediates and the ON rate kinetics of calcium binding, become practicable which were previously inaccessible. For a 10 nmol dm^{-3} concentration of TACaM a pseudo-first-order calcium binding rate constant of $< 10\ s^{-1}$ would be found if the bimolecular rate constant was diffusion controlled ($\approx 10^9\ dm^3\ mol^{-1}\ s^{-1}$, or less) which is measurable by a conventional kinetic stopped-flow apparatus.

The potential is being exploited in the study of calmodulin interactions and metastable intermediates with myosin light-chain kinase peptides.[54,55]

8. An additional asset of TACaM is its close similarity to the native calmodulin in many biochemical properties (*e.g.* calcium affinity of mean K_d *ca.* 500 nmol dm^{-3}, activation of MLCK, phosphodiesterases).

9. While the use of TACaM as an intracellular tracer of calmodulin and of the time and spatial course of calcium ion flux is feasible regarding sensitivity, a drawback for detailed quantitative studies lies in the bell-shaped function relating fluorescence intensity to calcium loading of the protein, which introduces an ambiguity regarding calcium level for a given fluorescence intensity.

In conclusion, this new fluorescent derivative of calmodulin TACaM reveals both the sequence of conformational changes on uptake of calcium ion at the major binding sites with clear indications of the key alterations in the region of the central helix expansion joint, and also provides a very sensitive reporter suitable for examination of the kinetics of interactions between calmodulin and target peptides.

Acknowledgements

We thank several people at NIMR, Mill Hill, London: P. M. Bayley in whose laboratory this work was initiated, S. R. Martin and K. Török for practical assistance in some optical measurements and in the isolation of calmodulin, respectively, also D. R. Trentham for constant encouragement in these studies. A support grant to D. J. Cowley for a visit to NIMR provided by the Nuffield Foundation, and a postdoctoral assistantship to J. P. McCormick from SERC are gratefully acknowledged.

References

1 D. J. Cowley, E. O'Kane and R. S. J. Todd, *J. Chem. Soc., Perkin Trans. 2*, 1991, 1495.
2 D. J. Cowley and R. S. J. Todd, *J. Chem. Soc., Perkin Trans. 2*, 1995, 299.
3 S. Forsen, H. J. Vogel, and T. Drakenberg, in *Calcium and Cell Function*, vol. VI, ed. W. Y. Cheung, Academic Press, New York, 1986, ch. 4.
4 Y. S. Babu, C. E. Bugg and W. J. Cook, in *Molecular Aspects of Cellular Recognition*, vol. 5, Calmodulin, eds. P. Cohen and C. B. Klee, Elsevier, Amsterdam, 1988, ch. 5.
5 C. D. Ramussen and A. R. Means, *TINS*, 1989, **12**, 433.
6 B. E. Finn and S. Forsen, *Structure*, 1995, **3**, 7.
7 G. Barbato, M. Ikura, L. E. Kay, R. W. Pastor and A. Bax, *Biochemistry*, 1992, **31**, 5269.
8 K. Török, A. N. Lane, S. R. Martin, J.-M. Janot and P. M. Bayley, *Biochemistry*, 1992, **31**, 3452.
9 A. Persechini and R. H. Kretsinger, *J. Biol. Chem.*, 1988, **263**, 12175.
10 R. H. Kretsinger, *Cell Calcium*, 1992, **13**, 363.
11 C. B. Klee, in *Calmodulin*, vol. 5, eds. P. Cohen and C. B. Klee, Elsevier, Amsterdam, 1988, pp. 35–56.
12 M. Zhang, T. Tanaka and M. Ikura, *Nature, Struct. Biol.*, 1995, **2**, 758.
13 H. Kuboniwa, N. Tjandra, S. Grzesiek, H. Ren, C. B. Klee and A. Bax, *Nature, Struct. Biol.*, 1995, **2**, 768.
14 B. E. Finn, J. Evenas, T. Drakenberg, J. P. Waltho, E. Thulin and S. Forsen, *Nature, Struct. Biol.*, 1995, **2**, 777.
15 M. Ikura, G. M. Clore, G. M. Gronenborn, A. M. Zhu, C. B. Klee and A. Bax, *Science*, 1992, **256**, 632.
16 S. M. Roth, D. M. Schneider, L. A. Strobel, M. F. A. Van Berkum, A. R. Means and A. J. Wand, *Biochemistry*, 1992, **31**, 1443.
17 W. E. Meador, A. R. Means and F. A. Quiocho, *Science*, 1992, **257**, 1251.
18 W. E. Meador, A. R. Means and F. A. Quiocho, *Science*, 1993, **262**, 1718.
19 W. E. Meador, S. E. George, A. R. Means and F. A. Quiocho, *Nature, Struct. Biol.*, 1995, **2**, 943.
20 J. Mackall and C. B. Klee, *Biochemistry*, 1991, **30**, 7242.
21 K. T. O'Neil and W. F. DeGrado, *Trends Biochem. Sci.*, 1990, **56**, 59.
22 J. L. Urbauer, J. H. Short, L. K. Dow and A. J. Wand, *Biochemistry*, 1995, **34**, 8099.
23 M. R. Ehrhardt, J. L. Urbauer and A. J. Wand, *Biochemistry*, 1995, **34**, 2731.
24 K. Török and M. Whitaker, *BioEssays*, 1994, **16**, 221.
25 W. A. Findlay, S. R. Martin, K. Beckingham and P. M. Bayley, *Biochemistry*, 1995, **34**, 2087.
26 M. Ikura, N. Hasegawa, S. Aimoto, M. Yazawa, K. Yagi and K. Hikichi, *Biochem. Biophys. Res. Commun.*, 1989, **161**, 1233.
27 A. Andersson, S. Forsen, E. Thulin and H. J. Vogel, *Biochemistry*, 1983, **22**, 2309.
28 S. R. Martin, A. Andersson Teleman, P. M. Bayley, T. Drakenberg and S. Forsen, *Eur. J. Biochem.*, 1985, **151**, 543.
29 J. Suko, W. Wyskovsky, J. Pidlich, R. Hauptner, B. Plank and G. Hellmann, *Eur. J. Biochem.*, 1986, **159**, 425.
30 S. Pedigo and M. A. Shea, *Biochemistry*, 1995, **34**, 10676.
31 M. Yizawa, T. Vorherr, P. James, E. Carafoli and K. Yagi, *Biochemistry*, 1992, **31**, 3171.
32 S. R. Martin, J. F. Maune, K. Beckingham and P. M. Bayley, *Eur. J. Biochem.*, 1992, **205**, 1107.
33 K. Beckingham, *J. Biol. Chem.*, 1991, **266**, 6027.
34 J. Haiech, M.-C. Kilhoffer, T. J. Lukas, T. A. Craig, D. M. Roberts and D. M. Watterson, *J. Biol. Chem.*, 1991, **266**, 3427.
35 Y. Waltersson, S. Linse, P. Brodin and T. Grundstrom, *Biochemistry*, 1993, **32**, 7866.
36 S. Pedigo and M. A. Shea, *Biochemistry*, 1995, **34**, 1179.
37 I. Durussel, J. A. Rhyner, E. E. Strehler and J. A. Cox, *Biochemistry*, 1993, **32**, 6089.
38 S. Ohki, U. Iwamoto, S. Aimoto, M. Yazawa and K. Hikichi, *J. Biol. Chem.*, 1993, **268**, 12388.
39 M. Milos, M. Comte, J.-J. Schaer and J. A. Cox, *J. Inorg. Biochem.*, 1989, **36**, 11.
40 D. Lafitte, J. P. Capony, G. Grassy, J. Haiech and B. Calas, *Biochemistry*, 1995, **34**, 13825.
41 M.-C. Kilhoffer, M. Kubina, F. Travers and J. Haiech, *Biochemistry*, 1992, **31**, 8098.
42 R. F. Steiner, L. Marshall and D. Needleman, *Biopolymers*, 1982, **25**, 351.
43 R. F. Steiner, P. K. Lambooy and H. Sternberg, *Arch. Biochem. Biophys.*, 1983, **222**, 158.
44 P. M. Bayley, S. R. Martin and G. Jones, *FEBS Lett.*, 1988, **238**, 61.
45 C.-L. A. Wang, *Biochemistry*, 1989, **28**, 4816.
46 E. R. Chapman, K. Alexander, T. Vorherr, E. Carafoli and D. R. Storm, *Biochemistry*, 1992, **31**, 12819.

47 J. S. Mills, M. P. Walsh, K. Nemcek and D. L. Johnson, *Biochemistry*, 1988, **27**, 991.
48 D. P. Giedroc, D. Puett, S. K. Sinha and K. Brew, *Arch. Biochem. Biophys.*, 1987, **252**, 136.
49 L. D. Dwyer, P. J. Crocker, D. S. Watt and T. C. Vanaman, *J. Biol. Chem.*, 1992, **267**, 22606.
50 B. B. Olwin and D. R. Storm, in *Methods in Enzymology*, vol. 102, Academic Press, New York, 1983, pp. 148–157.
51 F. M. Faust, M. Slisz and H. W. Jarrett, *J. Biol. Chem.*, 1987, **262**, 1938.
52 H. W. Jarrett, *J. Biol. Chem.*, 1984, **259**, 10136.
53 R. L. Kincaid, M. Vaughan, J. C. Osborne, Jr., *J. Biol. Chem.*, 1982, **257**, 10638.
54 K. Török, D. J. Cowley, B. D. Brandmeier, S. Howell, A. Aitken and D. R. Trentham, *Biochemistry*, in the press.
55 K. Török and D. R. Trentham, *Biochemistry*, 1994, **33**, 12807.
56 D. J. Cowley, *J. Chem. Soc., Perkin Trans. 2*, 1984, 281.
57 R. E. Dale, in *Time-resolved Fluorescence Spectroscopy in Biochemistry and Biology*, NATO A. S. I. Series A: Life Sciences, vol. 69A, eds. R. B. Cundall and R. E. Dale, Plenum Press, New York, 1983, pp. 508–9.
58 M. Comte, Y. Maulet and J. A. Cox, *Biochem. J.*, 1983, **209**, 269.
59 Y. Maulet and J. A. Cox, *Biochemistry*, 1983, **22**, 5680.
60 M. Itakura and T. Iio, *J. Biochem.*, 1992, **112**, 183.

Paper 6/00573J
Received 24*th January* 1996
Accepted 20*th March* 1996